An Overset Mesh Framework for an Isentropic ALE Navier-Stokes HDG Formulation

Justin A. Kauffman* and William L. George†
National Institute of Standards and Technology, Gaithersburg, MD 20899, USA

Jonathan S. Pitt‡
Virginia Polytechnic Institute and State University, Blacksburg, VA 24061, USA

Fluid-structure interaction simulations where solid bodies undergo large deformations require special handling of the mesh motion for Arbitrarily Lagrangian-Eulerian (ALE) formulations. Such formulations are necessary when body-fitted meshes with certain characteristics, such as boundary layer resolution, are required to properly resolve the problem. We present an overset mesh method to accommodate such problems in which flexible bodies undergo large deformations, or where rigid translation modes of motion occur. To accommodate these motions of the bodies through the computational domain, an overset mesh enabled ALE formulation for fluid flow is discretized with the hybridizable discontinuous Galerkin (HDG) finite element method. The overset mesh framework applied to the HDG method enables the deforming and translating dynamic meshes to maintain quality without remeshing. Verification is performed to demonstrate that optimal order convergence $\mathcal{O}(k+1)$ is obtained for arbitrary overlap and approximation order k.

I. Introduction

Developing numerical methods that can efficiently and accurately model complex multiphysics problems, such as fluid-structure interactions (FSI) where the bodies experience large deformations is still an active area of research. In order to capture large changes in the computational domain, which include solid deformations and/or rigid translation modes of motion, it is necessary to first study an arbitrarily Lagrangian-Eulerian (ALE) formulation of the governing fluid equations. This particular building block is of critical importance because we will employ a monolithic solver for FSI simulations [1], which requires that the governing fluid equations and governing solid equations be cast in the same reference frame. Further, an ALE formulation automatically allows for dynamic bodies, and therefore dynamic meshes to be incorporated. This last point is the driving motivation for utilizing an overset mesh framework. We have previously developed an overset mesh framework with the mathematical discretization of the hybridizable discontinuous Galerkin (HDG) finite element method for static linear problems such as convection-diffusion and elastostatics [2]. Below we present motivation for the use of an overset mesh method and the HDG method.

As physical geometries increase in complexity and bodies are required to move relative to one another throughout the duration of a simulation, choices must be made on how to discretize the computational domain. One approach is to decompose the domain into smaller subdomains, which we can allow to overlap, that can focus on the complex features and can maintain the initial mesh quality even as bodies move relative to one another. This approach has additional complications such as: How to address cells from a background mesh that lie within a solid body? How do meshes communicate with each other, especially in a case when multiple meshes overlap at the same location? The primary focus of this work is to demonstrate our communication algorithm between overset meshes.

Before proceeding it is necessary to define some common nomenclature that we will use in this work. We refer to a *mesh* as a discretized representation of a physical domain into polygonal volumes (i.e., cells). An *overset mesh* is a collection of meshes that overlap to discretize the entire physical domain. An *overset mesh method* uses overlapping meshes to discretize the physical domain. The first overset mesh method was developed by researchers at the National Aeronatics and Space Administration in 1983 [3, 4] to perform simulations of bodies in relative motion. Overset mesh methods have been applied to a variety of applications [5–11] for fixed and dynamic mesh scenarios.

*Postdoctoral Associate, National Institute of Standards and Technology, 100 Bureau Drive, MS 8911, Gaithersburg, MD 20899
†Computational Scientist, National Institute of Standards and Technology, 100 Bureau Drive, MS 8911, Gaithersburg, MD 20899
‡Research Associate Professor, Hume Center for National Security and Technology, Virginia Tech, 900 N. Glebe Rd., Arlington, VA 22203

Our communication algorithm provides an avenue for information to be transmitted from the interior of a *donor cell*, a cell that provides information to a different mesh, to an *acceptor cell*, which exists on an overset boundary. Fig. 1 shows two overset cells, a subset of two overset meshes, where in this example, the red cell is the acceptor and the blue cell is the donor. The edges of the cells that lie within the opposite cell are the *overset boundaries* and the purple points are *donor points* from the blue donor cell to the red acceptor cell.

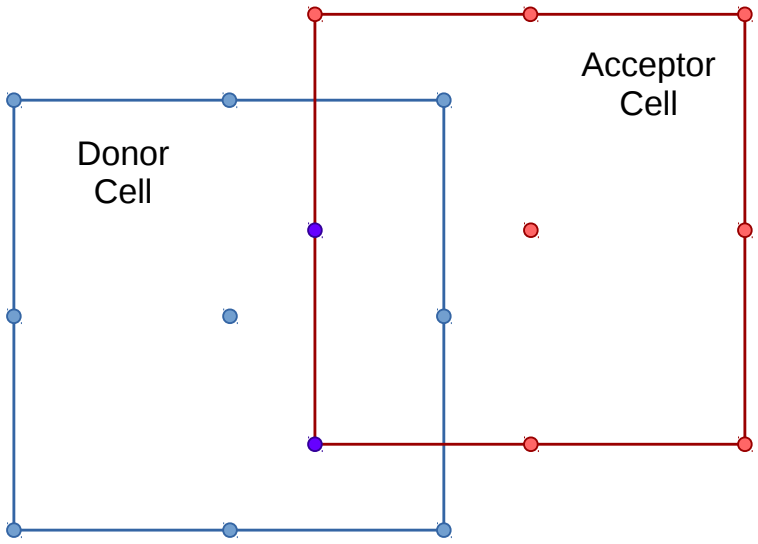

Fig. 1 The blue cell is a donor cell and the red cell is an acceptor cell. The purple points indicate where the basis functions of the blue cell will be evaluated to donate information to the red cell on that particular overset boundary. The points are distributed based on quadratic (Q2) discontinuous elements.

Higher-order finite difference and finite volume overset mesh methods require a larger overset region to maintain the higher-order approximations [12, 13]. This implies that more data must be stored, and also that the overset meshes must be manually constructed to ensure the correct amount of overlap during dynamic mesh motion applications is maintained. Nastase et al. [14] first remedied this problem by developing an overset discontinuous Galerkin (DG) approach for aerodynamic problems. The DG solver that replaced the finite difference solver is favorable because of the compact numerical stencil that results from this discretiztion. Similarly, Galbraith et al. [15] developed a DG Chimera scheme for solving the Euler and compressible Navier-Stokes equations. This scheme decomposes the computational domain into a set of structured overset meshes, which must at least abut to avoid gaps and voids in the domain. Communication via interpolation only occurs on the overset boundary faces, which is the same approach we are employing here and we first presented in [2]. The DG Chimera scheme also can handle mixed order meshes, so interpolation occurs between meshes of different approximation orders. Brazell et al. [16] also developed an overset DG approach within an overset mesh framework, `TIOGA` (Topology Independent Overset Grid Assembler). This approach performs interpolation over the entire overset boundary cell, instead of just the overset boundary face, which results in a different connectivity pattern compared to [15]. This DG-overset method investigates the Reynolds Averaged Naiver-Stokes equations with the Spalart-Allmaras turbulence model and utilizes unstructured mixed-element meshes. These DG-overset methods were the motivation to extend this concept to coupling overset meshes and the HDG finite element method.

The HDG method was first developed in [17] and provides an efficient way to reduce the size of the global system through the hybridization procedure. There have been previous HDG formulations for moving and deforming domains via an ALE perspective of the Navier-Stokes equations in Nguyen and Peraire [18] and Fidkowski [19]. The HDG ALE formulation has also been used to build an HDG FSI formulation in Sheldon et al. [1]. The HDG method has versatility and adaptability to enable straightforward implementation for a variety of different physics, which makes it ideal for complex multiphysics applications like FSI.

In the computational fluid dynamics (CFD) community DG methods are a viable alternative to finite volume methods, because this variant of the finite element method shares the conservation properties that are inherent to the finite volume method. Unfortunately, standard DG methods result in a linear system that becomes large due to duplication of degrees of freedom (DoFs) at nodes on element boundaries [18]. Through the hybridization process the global system is greatly reduced, when compared to standard DG methods, while maintaining the conservation properties that are necessary in

fluid dynamics. In Ahnert and Bärwolff [20] the authors compare an HDG method to a second-order finite volume method for incompressible flow; they conclude that the higher accuracy outweighs the slow matrix assembly for the HDG method compared to the finite volume method.

Hybridization involves introducing independent approximations on the border of elements (i.e., the trace of the elements) in addition to the interior of the elements for at least one field [21, Chapter 7]. Therefore, the new trace unknowns can be used to reduce the global system size and/or enrich the function space of the solutions. The HDG method decomposes the solution into two parts: the global solution trace, which exists on the cell boundaries, and the local solution, which exists internal to each cell. The local solution on each cell is only coupled with the global solution trace; therefore, the local solution on one cell is completely decoupled from the local solution of its neighboring cells. The only solution field that exists in both solution spaces is the hybrid unknown. The trace of the hybrid field approximates the global solution and is the only globally coupled field.

In this paper we are extending the overset mesh framework originally developed in [2] to an isentropic ALE Navier-Stokes HDG formulation. This formulation allows for bodies to move throughout the domain, relative to one another, and for the computational domain to deform. This paper serves as a proof-of-concept where we will verify our formulation using a four overset mesh configuration that demonstrates optimal order convergence is obtained for *arbitrary* overlap and *arbitrary* approximation order.

II. Governing Equations

In order to be incorporated in a monolithic solver the governing fluid equations are required to undergo a coordinate transformation from an Eulerian set of coordinates to an ALE set of coordinates. We describe this process below by first presenting the Eulerian form of the isentropic Navier-Stokes equations, where an equation of state for isentropic flow is

$$\frac{\partial \rho}{\partial t} = \beta \frac{\partial p}{\partial t}, \tag{1}$$

where $\beta = 1/c^2$ and c is the speed of sound through the fluid. Here we are neglecting the convective term from the material derivative and only relating the pure time derivatives, as in Bagwell [22]. Eq. (1) alters the continuity equation by incorporating time variance of pressure instead of density. The primary fields on the governing fluid system are velocity gradient $\mathbf{L}$, the velocity $\mathbf{v}$, and pressure p and the isentropic form of the governing Eulerian fluid equations over any physical domain Ω is

$$\mathbf{L} - \mathrm{grad}\mathbf{v} = \mathbf{0}, \qquad \forall \boldsymbol{x} \in \Omega, \tag{2a}$$

$$\rho \frac{\partial \mathbf{v}}{\partial t} + \mathrm{div}\left(-\mu \mathbf{L} + p\mathbf{I}\right) + \rho \mathbf{L}\mathbf{v} + \rho\left(\mathrm{div}\mathbf{v}\right)\mathbf{v} = \mathbf{f}, \qquad \forall \boldsymbol{x} \in \Omega, \tag{2b}$$

$$\varepsilon \frac{\partial p}{\partial t} + \mathrm{div}\mathbf{v} = 0, \qquad \forall \boldsymbol{x} \in \Omega, \tag{2c}$$

$$\left(-\mu \mathbf{L} + p\mathbf{I}\right)\mathbf{n} = \mathbf{g}_N, \quad \forall \boldsymbol{x} \in \partial\Omega_N, \tag{2d}$$

$$\mathbf{v} = \mathbf{g}_D, \quad \forall \boldsymbol{x} \in \partial\Omega_D, \tag{2e}$$

where $\varepsilon = \beta/\rho$, $\mathbf{g}_N$ is a prescribed traction on $\partial\Omega_N$, and $\mathbf{g}_D$ is a prescribed velocity on $\partial\Omega_D$. In order to reformulate Eq. (2) to an ALE perspective we require the use of the mesh displacment $\mathbf{u}_\mathrm{m}$ and the mesh deformation gradient $\mathbf{F}_\mathrm{m}$ through the following relations

$$\mathbf{F}_\mathrm{m} = \mathbf{I} + \mathrm{Grad}\mathbf{u}_\mathrm{m}, \tag{3a}$$

$$\mathrm{grad}p = \mathbf{F}_\mathrm{m}^{-\mathsf{T}}\mathrm{Grad}p, \tag{3b}$$

$$\mathrm{grad}\mathbf{v} = \left(\mathrm{Grad}\mathbf{v}\right)\mathbf{F}_\mathrm{m}^{-1}, \tag{3c}$$

$$\mathrm{div}\mathbf{L} = \mathrm{Grad}\mathbf{L} : \mathbf{F}_\mathrm{m}^{-\mathsf{T}}, \tag{3d}$$

$$\mathrm{div}\mathbf{v} = \mathrm{Grad}\mathbf{v} : \mathbf{F}_\mathrm{m}^{-\mathsf{T}}, \tag{3e}$$

where the subscript m indicates that the field corresponds to the governing equations of the mesh. Also, the $:$ operator in Eqs. (3d) and (3e) is a double contraction [23] meaning that two indices are summed over and results in a scalar field if $:$ acts between two second order tensors (as in Eq. (3e)), or in a vector if $:$ acts between a third order tensor and a second order tensor (as in Eq. (3d)). We should note that grad and Grad are distinguished based on the coordinates,

and therefore the reference configuration, that these derivatives are being performed on, namely grad $:= \partial/\partial \boldsymbol{x}$ and Grad $:= \partial/\partial \mathbf{X}$, which is consistent with [24]. Additionally, we need the so-called 'fundamental ALE equation' [25] in both scalar and vector form:

$$\phi' = \dot{\phi} - \mathbf{F}_{\mathrm{m}}^{-\mathsf{T}} \mathrm{Grad}\phi \cdot \frac{\partial \mathbf{X}}{\partial t}, \tag{4a}$$

$$\mathbf{a}' = \dot{\mathbf{a}} - \left[(\mathrm{Grad}\mathbf{a})\, \mathbf{F}_{\mathrm{m}}^{-1} \right] \frac{\partial \mathbf{X}}{\partial t}, \tag{4b}$$

where $\partial \mathbf{X}/\partial t = \mathbf{v}_{\mathrm{m}}$, the mesh velocity, the prime derivative is a material time derivative, and the dot derivative is an ordinary time derivative ($\partial/\partial t$). Lastly, normal vectors viewed from the ALE perspective instead of the Eulerian perspective undergo the following transformation

$$\mathbf{n} = \mathbf{F}_{\mathrm{m}}^{-\mathsf{T}} \mathbf{n}_{\mathrm{f}}, \tag{5}$$

where $\mathbf{n}$ is the original fluid normal vector in the Eulerian reference frame and $\mathbf{n}_{\mathrm{f}}$ is the fluid normal vector in the ALE reference frame. Using Eqs. (2)–(5) we can obtain the isentropic form of the governing ALE equations. This governing system contains two parts, the governing fluid equations and the governing mesh equations. The partial differential equations (PDE) system governing the fluid mechanics, which consists of primary fields velocity gradient $\mathbf{L}_{\mathrm{f}}$, velocity $\mathbf{v}_{\mathrm{f}}$, and pressure p_{f} is

$$\mathbf{L}_{\mathrm{f}} - \mathrm{Grad}\mathbf{v}_{\mathrm{f}} \mathbf{F}_{\mathrm{m}}^{-1} = \mathbf{0}, \qquad \forall \mathbf{X} \in \Omega_{\mathrm{F}}(0), \tag{6a}$$

$$\rho_{\mathrm{f}} \frac{\partial \mathbf{v}_{\mathrm{f}}}{\partial t} + \rho_{\mathrm{f}} \mathbf{L}_{\mathrm{f}} (\mathbf{v}_{\mathrm{f}} - \mathbf{v}_{\mathrm{m}}) - \mu_{\mathrm{f}} \mathrm{Grad}\mathbf{L}_{\mathrm{f}} : \mathbf{F}_{\mathrm{m}}^{-\mathsf{T}} + \mathbf{F}_{\mathrm{m}}^{-\mathsf{T}} \mathrm{Grad} p_{\mathrm{f}} + \rho_{\mathrm{f}} \left(\mathrm{Grad}\mathbf{v}_{\mathrm{f}} : \mathbf{F}_{\mathrm{f}}^{-\mathsf{T}} \right) \mathbf{v}_{\mathrm{f}} = \mathbf{f}_{\mathrm{f}}, \qquad \forall \mathbf{X} \in \Omega_{\mathrm{F}}(0), \tag{6b}$$

$$\varepsilon \frac{\partial p_{\mathrm{f}}}{\partial t} - \varepsilon \left[\mathbf{F}_{\mathrm{m}}^{-\mathsf{T}} \mathrm{Grad} p_{\mathrm{f}} \right] \cdot \mathbf{v}_{\mathrm{m}} + \mathrm{Grad}\mathbf{v}_{\mathrm{f}} : \mathbf{F}_{\mathrm{m}}^{-\mathsf{T}} = 0, \qquad \forall \mathbf{X} \in \Omega_{\mathrm{F}}(0), \tag{6c}$$

$$(-\mu_{\mathrm{f}} \mathbf{L}_{\mathrm{f}} + p_{\mathrm{f}} \mathbf{I})\, \mathbf{F}_{\mathrm{m}}^{-\mathsf{T}} \mathbf{n}_{\mathrm{f}} = \mathbf{g}_{N_{\mathrm{f}}}, \quad \forall \mathbf{X} \in \partial\Omega_{N_{\mathrm{F}}}(0), \tag{6d}$$

$$\mathbf{v}_{\mathrm{f}} = \mathbf{g}_{D_{\mathrm{f}}}, \quad \forall \mathbf{X} \in \partial\Omega_{D_{\mathrm{F}}}(0), \tag{6e}$$

where $\Omega_{\mathrm{F}}(0)$ is the initial physical fluid domain from the ALE perspective. The fields that are required in order to couple the fluid and mesh together are the deformation gradient $\mathbf{F}_{\mathrm{m}}$ and the mesh velocity $\mathbf{v}_{\mathrm{m}}$. The mesh velocity is not a primary field in the mesh governing system, but it is approximated via a backward difference of the mesh displacement $\mathbf{u}_{\mathrm{m}}$ in time [26]. The mesh motion is governed by an elastostatics formulation; therefore, we do not consider elastic wave propagation and the mesh PDE system is time-independent, but a mesh velocity can be approximated through the change in displacement. The PDE system governing the mesh motion, which consists of primary fields displacement $\mathbf{u}_{\mathrm{m}}$ and deformation gradient $\mathbf{F}_{\mathrm{m}}$ is

$$\mathbf{F}_{\mathrm{m}} - \mathbf{I} - \mathrm{Grad}\mathbf{u}_{\mathrm{m}} = \mathbf{0}, \qquad \forall \mathbf{X} \in \Omega_{\mathrm{F}}(0), \tag{7a}$$

$$-\mathrm{Div}\left[\mathbb{C} (\mathrm{Sym}\mathbf{F}_{\mathrm{m}} - \mathbf{I}) \right] = \mathbf{b}_{\mathrm{m}}, \qquad \forall \mathbf{X} \in \Omega_{\mathrm{F}}(0), \tag{7b}$$

$$\mathbb{C} (\mathrm{Sym}\mathbf{F}_{\mathrm{m}} - \mathbf{I})\, \mathbf{n}_{\mathrm{m}} = \mathbf{t}_{N_{\mathrm{m}}}, \quad \forall \mathbf{X} \in \partial\Omega_{N_{\mathrm{F}}}(0), \tag{7c}$$

$$\mathbf{u}_{\mathrm{m}} = \bar{\mathbf{u}}_{D_{\mathrm{m}}}, \quad \forall \mathbf{X} \in \partial\Omega_{D_{\mathrm{F}}}(0), \tag{7d}$$

where $\mathbb{C}$ is the fourth order elasticity tensor, $\mathrm{Sym}\mathbf{F}_{\mathrm{m}} = 1/2 \left(\mathbf{F}_{\mathrm{m}} + \mathbf{F}_{\mathrm{m}}^{\mathsf{T}} \right)$, and $\mathbf{b}_{\mathrm{m}}$ is a source term in the balance of linear momentum. In order to present the variational (or weak) forms of Systems (6) and (7) we need to describe the relationship between the differential volume/area elements as we change our reference frame from Eulerian to ALE. This relation is

$$dv = J_{\mathrm{m}}^{\mathrm{h}} dv_{\mathrm{m}}, \quad da = J_{\mathrm{m}}^{\mathrm{h}} da_{\mathrm{m}}, \tag{8}$$

where $J_{\mathrm{m}}^{\mathrm{h}} = \det \mathbf{F}_{\mathrm{m}}^{\mathrm{h}}$. Since the weak form is a set of integral equations the differentials used in those integrals need to undergo the changes defined in Eq. (8).

III. Overset Hybridizable Discontinuous Galerkin Method

We have already written Systems (6) and (7) in first-order form since it is required for the HDG method. Before discretizing the aforementioned governing PDE systems we need to introduce some notation that will be used throughout

Table 1 Notation utilized in the HDG finite element method.

Notation	Description
d	The spatial degree of the problem $\{d = 2, 3\}$.
$\mathscr{T}_\mathrm{h}$	The entire computational domain.
N	Total number of meshes used to discretely describe $\mathscr{T}_\mathrm{h}$.
i	The mesh id number.
$\mathcal{T}_\mathrm{h}^i$	The discretized i^{th} computational domain (or triangulation).
$\partial\mathcal{T}_\mathrm{h}^i$	The union of all faces of domain $\mathcal{T}_\mathrm{h}^i$.
K	An individual cell in $\mathcal{T}_\mathrm{h}^i$.
∂K	The boundary of an individual cell.
F	The face of a cell.
$\mathcal{F}_\mathrm{h}^i$	Set of all faces, for all cells in $\mathcal{T}_\mathrm{h}^i$.
$P_k(K)$	Space of polynomials of degree $\leq k$ over K.
$P_k(F)$	Space of polynomials of degree $\leq k$ over F.

the rest of this paper. First, Table 1 describes common definitions that we will use. Note that $\mathscr{T}_\mathrm{h} = \bigcup_{i=1}^{N} \mathcal{T}_\mathrm{h}^i$. We also must define the local and global inner products. The local inner products are over cells

$$(a,b)_K := \int_K ab, \qquad \langle a,b\rangle_{\partial K} := \int_{\partial K} ab, \qquad \text{for scalars,} \tag{9a}$$

$$(\mathbf{a},\mathbf{b})_K := \int_K \mathbf{a}\cdot\mathbf{b}, \qquad \langle \mathbf{a},\mathbf{b}\rangle_{\partial K} := \int_{\partial K} \mathbf{a}\cdot\mathbf{b}, \qquad \text{for vectors,} \tag{9b}$$

$$(\mathbf{A},\mathbf{B})_K := \int_K \mathbf{A}:\mathbf{B}, \qquad \langle \mathbf{A},\mathbf{B}\rangle_{\partial K} := \int_{\partial K} \mathbf{A}:\mathbf{B}, \qquad \text{for tensors,} \tag{9c}$$

whereas the global inner products are over the entire discretized domain

$$(a,b)_{\mathcal{T}_\mathrm{h}^i} := \sum_K (a,b)_K, \qquad \langle a,b\rangle_{\partial\mathcal{T}_\mathrm{h}^i} := \sum_{\partial K} (a,b)_{\partial K}, \qquad \text{for scalars,} \tag{10a}$$

$$(\mathbf{a},\mathbf{b})_{\mathcal{T}_\mathrm{h}^i} := \sum_K (\mathbf{a},\mathbf{b})_K, \qquad \langle \mathbf{a},\mathbf{b}\rangle_{\partial\mathcal{T}_\mathrm{h}^i} := \sum_{\partial K} (\mathbf{a},\mathbf{b})_{\partial K}, \qquad \text{for vectors,} \tag{10b}$$

$$(\mathbf{A},\mathbf{B})_{\mathcal{T}_\mathrm{h}^i} := \sum_K (\mathbf{A},\mathbf{B})_K, \qquad \langle \mathbf{A},\mathbf{B}\rangle_{\partial\mathcal{T}_\mathrm{h}^i} := \sum_{\partial K} (\mathbf{A},\mathbf{B})_{\partial K}, \qquad \text{for tensors.} \tag{10c}$$

Finally, we introduce the local discontinuous approximation spaces as

$$\mathscr{G}_\mathrm{h} := \left\{ \mathbf{G}^\mathrm{h} \in \left[L^2\left(\mathcal{T}_\mathrm{h}^i\right)\right]^{d\times d} : \mathbf{G}^\mathrm{h}|_K \in [P_k(K)]^{d\times d},\ \forall K \in \mathcal{T}_\mathrm{h}^i,\ \forall i \right\}, \tag{11a}$$

$$\mathscr{Y}_\mathrm{h} := \left\{ \mathbf{y}^\mathrm{h} \in \left[H^1\left(\mathcal{T}_\mathrm{h}^i\right)\right]^{d} : \mathbf{y}^\mathrm{h}|_K \in [P_k(K)]^{d},\ \forall K \in \mathcal{T}_\mathrm{h}^i,\ \forall i \right\}, \tag{11b}$$

$$\mathscr{P}_\mathrm{h} := \left\{ q^\mathrm{h} \in L^2\left(\mathcal{T}_\mathrm{h}^i\right) : q^\mathrm{h}|_K \in P_k(K),\ \forall K \in \mathcal{T}_\mathrm{h}^i,\ \forall i \right\}, \tag{11c}$$

$$\mathscr{C}_\mathrm{h} := \left\{ \mathbf{C}^\mathrm{h} \in \left[L^2\left(\mathcal{T}_\mathrm{h}^i\right)\right]^{d\times d} : \mathbf{C}^\mathrm{h}|_K \in [P_k(K)]^{d\times d},\ \forall K \in \mathcal{T}_\mathrm{h}^i,\ \forall i \right\}, \tag{11d}$$

$$\mathscr{U}_\mathrm{h} := \left\{ \mathbf{w}^\mathrm{h} \in \left[H^1\left(\mathcal{T}_\mathrm{h}^i\right)\right]^{d} : \mathbf{w}^\mathrm{h}|_K \in [P_k(K)]^{d},\ \forall K \in \mathcal{T}_\mathrm{h}^i,\ \forall i \right\}, \tag{11e}$$

where the L^2 is a Hilbert space where functions are square Lebesgue integrable and H^1 is a Sobolev space where the first order weak derivatives of a function exists. Additionally, we also have to introduce two approximation spaces for

the global fields, i.e., the trace of the solutions. Each system requires its own solution trace (velocity for the fluid system and displacement for the mesh system). The discontinuous approximation spaces for the global fields are

$$\mathscr{N}_{\mathrm{h}} \coloneqq \left\{ \eta^{\mathrm{h}} \in \left[L^2\left(\mathcal{F}_{\mathrm{h}}^i\right)\right]^d : \eta^{\mathrm{h}}|_F \in [P_k(F)]^d,\ \forall F \in \mathcal{F}_{\mathrm{h}}^i,\ \forall K \in \mathcal{T}_{\mathrm{h}}^i,\ \forall i \right\}, \tag{12a}$$

$$\mathscr{M}_{\mathrm{h}} \coloneqq \left\{ \omega^{\mathrm{h}} \in \left[L^2\left(\mathcal{F}_{\mathrm{h}}^i\right)\right]^d : \omega^{\mathrm{h}}|_F \in [P_k(F)]^d,\ \forall F \in \mathcal{F}_{\mathrm{h}}^i,\ \forall K \in \mathcal{T}_{\mathrm{h}}^i,\ \forall i \right\}. \tag{12b}$$

A. Overset Framework

For an overset mesh framework the physical domain is decomposed into N subdomains that must at least abut, but will overlap in general. Mathematically, this decomposition is

$$\Omega = \Omega^1 \cup \Omega^2 \cup \cdots \cup \Omega^N \tag{13}$$

Domains are considered to overlap if

$$\Omega^i \cap \Omega^j \neq \emptyset, \quad \text{for any } i, j \in \{1, \ldots, N\}, \quad i \neq j, \tag{14}$$

and considered to abut if they share a common boundary, but do not otherwise overlap, namely,

$$\overline{\Omega}^i \cap \overline{\Omega}^j \neq \emptyset, \quad \Omega^i \cap \Omega^j = \emptyset, \quad \text{for any } i, j \in \{1, \ldots, N\}, \quad i \neq j. \tag{15}$$

Communication between the overset meshes is achieved via local (interior/volume) field information being donated from one domain to the face/edge of another domain on integrals over the overset boundaries (the purple points in Figure 1 where the interior information is being donated from the blue cell). The coupling between domains is a face-volume, or global-local, coupling which occurs naturally in the HDG method. Also, as we will show in Section III.B the local problem, which is solved on each cell K in each $\mathcal{T}_{\mathrm{h}}^i$, does not change. More details about the linear algebra are provided in Section III.C. Donated fields will be represented with a breve accent, $\breve{p}$ for example. This implies that the local field contributions to the integrals on the overset boundaries have information from the interior of a different mesh being included (i.e., donated).

B. Overset Formulation

The weak form of the isentropic ALE Navier-Stokes problem in an overset mesh framework is obtained by multiplying each equation in Systems (6) and (7) by a corresponding test function and then integrating over each cell in each domain. The test functions are $\{\mathbf{G}, \mathbf{y}, q\}$ for the fluid system and $\{\mathbf{C}, \mathbf{w}\}$ for the mesh system. We used integration by parts to obtain boundary terms on each element in order to define the numerical traces between cells. The local weak form is obtained by observing one cell $K \in \mathcal{T}_{\mathrm{h}}^i$ such that the following is satisfied:

Local Problem 1 (Local Isentropic ALE Navier-Stokes) *Find* $\left(\mathbf{L}_{\mathrm{f}}^{\mathrm{h}}, \mathbf{v}_{\mathrm{f}}^{\mathrm{h}}, p_{\mathrm{f}}^{\mathrm{h}}, \mathbf{F}_{\mathrm{m}}^{\mathrm{h}}, \mathbf{u}_{\mathrm{m}}^{\mathrm{h}}\right) \in \mathscr{G}_{\mathrm{h}} \times \mathscr{Y}_{\mathrm{h}} \times \mathscr{P}_{\mathrm{h}} \times \mathscr{C}_{\mathrm{h}} \times \mathscr{U}_{\mathrm{h}}$ *such that*

Local Subproblem 1.1 (Fluid)

$$\left(\mathbf{G}, J_{\mathrm{m}}^{\mathrm{h}} \mathbf{L}_{\mathrm{f}}^{\mathrm{h}}\right)_K - \left(\mathbf{G}, J_{\mathrm{m}}^{\mathrm{h}} \mathrm{Grad}\mathbf{v}_{\mathrm{f}}^{\mathrm{h}} \mathbf{F}_{\mathrm{m}}^{-1}\right)_K + \left\langle \mathbf{G}, J_{\mathrm{m}}^{\mathrm{h}} \left(\mathbf{v}_{\mathrm{f}}^{\mathrm{h}} - \widehat{\mathbf{v}}_{\mathrm{f}}^{\mathrm{h}}\right) \otimes \mathbf{F}_{\mathrm{m}}^{-\mathsf{T}} \mathbf{n}_{\mathrm{f}} \right\rangle_{\partial K} = 0, \tag{16a}$$

$$\begin{aligned} \left(\mathbf{y}, J_{\mathrm{m}}^{\mathrm{h}} \rho_{\mathrm{f}} \frac{\partial \mathbf{v}_{\mathrm{f}}^{\mathrm{h}}}{\partial t}\right)_K + \left(\mathbf{y}, J_{\mathrm{m}}^{\mathrm{h}} \rho_{\mathrm{f}} \mathbf{L}_{\mathrm{f}}^{\mathrm{h}} \left[\mathbf{v}_{\mathrm{f}}^{\mathrm{h}} - \mathbf{v}_{\mathrm{m}}^{\mathrm{h}}\right]\right)_K + \left(\mathrm{Grad}\mathbf{y}, J_{\mathrm{m}}^{\mathrm{h}} \left[\mu_{\mathrm{f}} \mathbf{L}_{\mathrm{f}}^{\mathrm{h}} - p_{\mathrm{f}}^{\mathrm{h}} \mathbf{I}\right] \mathbf{F}_{\mathrm{m}}^{-\mathsf{T}}\right)_K \\ + \left(\mathbf{y}, J_{\mathrm{m}}^{\mathrm{h}} \rho_{\mathrm{f}} \left[\mathrm{Grad}\mathbf{v}_{\mathrm{f}}^{\mathrm{h}} : \mathbf{F}_{\mathrm{m}}^{-\mathsf{T}}\right] \mathbf{v}_{\mathrm{f}}^{\mathrm{h}}\right)_K + \left\langle \mathbf{y}, J_{\mathrm{m}}^{\mathrm{h}} \widehat{\mathbf{T}}_{\mathrm{f}}^{\mathrm{h}} \mathbf{F}_{\mathrm{m}}^{-\mathsf{T}} \mathbf{n}_{\mathrm{f}} \right\rangle_{\partial K} = \left(\mathbf{y}, J_{\mathrm{m}}^{\mathrm{h}} \mathbf{f}_{\mathrm{f}}\right)_K, \end{aligned} \tag{16b}$$

$$\left(q, J_{\mathrm{m}}^{\mathrm{h}} \varepsilon \frac{\partial p_{\mathrm{f}}^{\mathrm{h}}}{\partial t}\right)_K + \left(q, J_{\mathrm{m}}^{\mathrm{h}} \varepsilon \left[\mathbf{F}_{\mathrm{m}}^{-\mathsf{T}} \mathrm{Grad} p_{\mathrm{f}}^{\mathrm{h}}\right] \cdot \mathbf{v}_{\mathrm{m}}^{\mathrm{h}}\right)_K - \left(\mathrm{Grad}q, J_{\mathrm{m}}^{\mathrm{h}} \mathbf{F}_{\mathrm{m}}^{-1} \mathbf{v}_{\mathrm{f}}^{\mathrm{h}}\right)_K + \left\langle q, J_{\mathrm{m}}^{\mathrm{h}} \widehat{\mathbf{v}}_{\mathrm{f}}^{\mathrm{h}} \cdot \mathbf{F}_{\mathrm{m}}^{-\mathsf{T}} \mathbf{n}_{\mathrm{f}} \right\rangle_{\partial K} = 0, \tag{16c}$$

where

$$\widehat{\mathbf{T}}_{\mathrm{f}}^{\mathrm{h}} \mathbf{F}_{\mathrm{m}}^{-\mathsf{T}} \mathbf{n}_{\mathrm{f}} \coloneqq \left[-\mu_{\mathrm{f}} \mathbf{L}_{\mathrm{f}}^{\mathrm{h}} + p_{\mathrm{f}}^{\mathrm{h}} \mathbf{I}\right] \mathbf{F}_{\mathrm{m}}^{-\mathsf{T}} \mathbf{n}_{\mathrm{f}} + \mathbf{S}_{\mathrm{f}} \left(\mathbf{v}_{\mathrm{f}}^{\mathrm{h}} - \widehat{\mathbf{v}}_{\mathrm{f}}^{\mathrm{h}}\right), \tag{17}$$

Local Subproblem 1.2 (Mesh Motion)

$$\left(\mathbf{C}, \mathbf{F}_{\mathrm{m}}^{\mathrm{h}} - \mathbf{I}\right)_K - \left(\mathbf{C}, \mathrm{Grad}\mathbf{u}_{\mathrm{m}}^{\mathrm{h}}\right)_K - \left\langle \mathbf{C}\mathbf{n}_{\mathrm{m}}, \left(\mathbf{u}_{\mathrm{m}}^{\mathrm{h}} - \widehat{\mathbf{u}}_{\mathrm{m}}^{\mathrm{h}}\right)\right\rangle_{\partial K} = 0, \tag{18a}$$

$$\left(\mathrm{Grad}\mathbf{w}, \mathbb{C}\left[\mathrm{Sym}\mathbf{F}_{\mathrm{m}}^{\mathrm{h}} - \mathbf{I}\right]\right)_K - \left\langle \mathbf{w}, \widehat{\mathbf{P}}_{\mathrm{m}}^{\mathrm{h}}\mathbf{n}_{\mathrm{m}}\right\rangle_{\partial K} = (\mathbf{w}, \mathbf{b}_{\mathrm{m}})_K, \tag{18b}$$

where

$$\widehat{\mathbf{P}}_{\mathrm{m}}^{\mathrm{h}}\mathbf{n}_{\mathrm{m}} := \mathbb{C}\left(\mathrm{Sym}\mathbf{F}_{\mathrm{m}}^{\mathrm{h}} - \mathbf{I}\right)\mathbf{n}_{\mathrm{m}} - \mathbf{S}_{\mathrm{m}}\left(\mathbf{u}_{\mathrm{m}}^{\mathrm{h}} - \widehat{\mathbf{u}}_{\mathrm{m}}^{\mathrm{h}}\right), \tag{19}$$

$\forall\, (\mathbf{G}, \mathbf{y}, q, \mathbf{C}, \mathbf{w}) \in \mathscr{G}_{\mathrm{h}} \times \mathscr{Y}_{\mathrm{h}} \times \mathscr{P}_{\mathrm{h}} \times \mathscr{C}_{\mathrm{h}} \times \mathscr{U}_{\mathrm{h}}$,

where $\mathbf{S}_{\mathrm{f}}$ and $\mathbf{S}_{\mathrm{m}}$ are second order stabilization tensors, which are defined as

$$\mathbf{S}_{\mathrm{f}} := \left(2\mu_{\mathrm{f}} + \rho_{\mathrm{f}}\|\mathbf{v}_{\mathrm{f}}^{\mathrm{h}}\|\right)\mathbf{I}, \tag{20a}$$

$$\mathbf{S}_{\mathrm{m}} := 50\mu_{\mathrm{m}}\mathbf{I}, \tag{20b}$$

where $\|\cdot\|$ represents the standard L^2-norm, μ_{m} is the shear modulus of the linear elastic mesh motion, and that the factor of 50 in the definition of $\mathbf{S}_{\mathrm{m}}$ is for increased stability and convergence. The definition of $\mathbf{S}_{\mathrm{f}}$ is based off of the work by Sheldon et al. [1].

Local Problem 1 is then discretized in time using a third order backward difference formula (BDF3) [26]. This formula is

$$11y^n - 18y^{n-1} + 9y^{n-2} - 2y^{n-3} = 6\Delta t f\left(t^n\right). \tag{21}$$

The fully discrete local weak form is provided in the Appendix. After discretizing in time, it is possible to solve Local Problem 1, which is composed of Local Subproblem 1.1 and Local Subproblem 1.2, if the numerical traces $\widehat{\mathbf{v}}_{\mathrm{f}}^{\mathrm{h}}$ and $\widehat{\mathbf{u}}_{\mathrm{m}}^{\mathrm{h}}$ are known. To determine the solutions of the numerical traces we have to sum over all K, in each $\mathcal{T}_{\mathrm{h}}^i$, and enforce the boundary conditions and continuity of the numerical traces $\left\langle \mathbf{y}, J_{\mathrm{m}}^{\mathrm{h}}\widehat{\mathbf{T}}_{\mathrm{f}}^{\mathrm{h}}\mathbf{F}_{\mathrm{m}}^{-\mathsf{T}}\mathbf{n}_{\mathrm{f}}\right\rangle_{\partial K}$ and $\left\langle \mathbf{w}, \widehat{\mathbf{P}}_{\mathrm{m}}^{\mathrm{h}}\mathbf{n}_{\mathrm{m}}\right\rangle_{\partial K}$ where $\widehat{\mathbf{T}}_{\mathrm{f}}^{\mathrm{h}}\mathbf{F}_{\mathrm{m}}^{-\mathsf{T}}\mathbf{n}_{\mathrm{f}}$ and $\widehat{\mathbf{P}}_{\mathrm{m}}^{\mathrm{h}}\mathbf{n}_{\mathrm{m}}$ are defined in Eq. (17) and (19). The resulting weak form is

Problem 1 (Global Isentropic ALE Navier-Stokes) *Find* $\left(\mathbf{L}_{\mathrm{f}}^{\mathrm{h}}, \mathbf{v}_{\mathrm{f}}^{\mathrm{h}}, p_{\mathrm{f}}^{\mathrm{h}}, \widehat{\mathbf{v}}_{\mathrm{f}}^{\mathrm{h}}, \mathbf{F}_{\mathrm{m}}^{\mathrm{h}}, \mathbf{u}_{\mathrm{m}}^{\mathrm{h}}, \widehat{\mathbf{u}}_{\mathrm{m}}^{\mathrm{h}}\right) \in \mathscr{G}_{\mathrm{h}} \times \mathscr{Y}_{\mathrm{h}} \times \mathscr{P}_{\mathrm{h}} \times \mathscr{N}_{\mathrm{h}} \times \mathscr{C}_{\mathrm{h}} \times \mathscr{U}_{\mathrm{h}} \times \mathscr{M}_{\mathrm{h}}$ *such that*

Subproblem 1.1 (Fluid)

$$\left(\mathbf{G}, J_{\mathrm{m}}^{\mathrm{h}}\mathbf{L}_{\mathrm{f}}^{\mathrm{h}}\right)_{\mathscr{T}_{\mathrm{h}}} - \left(\mathbf{G}, J_{\mathrm{m}}^{\mathrm{h}}\mathrm{Grad}\mathbf{v}_{\mathrm{f}}^{\mathrm{h}}\mathbf{F}_{\mathrm{m}}^{-1}\right)_{\mathscr{T}_{\mathrm{h}}} + \left\langle \mathbf{G}, J_{\mathrm{m}}^{\mathrm{h}}\left(\mathbf{v}_{\mathrm{f}}^{\mathrm{h}} - \widehat{\mathbf{v}}_{\mathrm{f}}^{\mathrm{h}}\right) \otimes \mathbf{F}_{\mathrm{m}}^{-\mathsf{T}}\mathbf{n}_{\mathrm{f}}\right\rangle_{\partial\mathscr{T}_{\mathrm{h}}} = 0, \tag{22a}$$

$$\left(\mathbf{y}, J_{\mathrm{m}}^{\mathrm{h}}\rho_{\mathrm{f}}\frac{\partial\mathbf{v}_{\mathrm{f}}^{\mathrm{h}}}{\partial t}\right)_{\mathscr{T}_{\mathrm{h}}} + \left(\mathbf{y}, J_{\mathrm{m}}^{\mathrm{h}}\rho_{\mathrm{f}}\mathbf{L}_{\mathrm{f}}^{\mathrm{h}}\left[\mathbf{v}_{\mathrm{f}}^{\mathrm{h}} - \mathbf{v}_{\mathrm{m}}^{\mathrm{h}}\right]\right)_{\mathscr{T}_{\mathrm{h}}} + \left(\mathrm{Grad}\mathbf{y}, J_{\mathrm{m}}^{\mathrm{h}}\left[\mu_{\mathrm{f}}\mathbf{L}_{\mathrm{f}}^{\mathrm{h}} - p_{\mathrm{f}}^{\mathrm{h}}\mathbf{I}\right]\mathbf{F}_{\mathrm{m}}^{-\mathsf{T}}\right)_{\mathscr{T}_{\mathrm{h}}}$$
$$+ \left(\mathbf{y}, J_{\mathrm{m}}^{\mathrm{h}}\rho_{\mathrm{f}}\left[\mathrm{Grad}\mathbf{v}_{\mathrm{f}}^{\mathrm{h}} : \mathbf{F}_{\mathrm{m}}^{-\mathsf{T}}\right]\mathbf{v}_{\mathrm{f}}^{\mathrm{h}}\right)_{\mathscr{T}_{\mathrm{h}}} + \left\langle \mathbf{y}, J_{\mathrm{m}}^{\mathrm{h}}\widehat{\mathbf{T}}_{\mathrm{f}}^{\mathrm{h}}\mathbf{F}_{\mathrm{m}}^{-\mathsf{T}}\mathbf{n}_{\mathrm{f}}\right\rangle_{\partial\mathscr{T}_{\mathrm{h}}} - \left(\mathbf{y}, J_{\mathrm{m}}^{\mathrm{h}}\mathbf{f}_{\mathrm{f}}\right)_{\mathscr{T}_{\mathrm{h}}} = 0, \tag{22b}$$

$$\left(q, J_{\mathrm{m}}^{\mathrm{h}}\varepsilon\frac{\partial p_{\mathrm{f}}^{\mathrm{h}}}{\partial t}\right)_{\mathscr{T}_{\mathrm{h}}} + \left(q, J_{\mathrm{m}}^{\mathrm{h}}\varepsilon\left[\mathbf{F}_{\mathrm{m}}^{-\mathsf{T}}\mathrm{Grad}p_{\mathrm{f}}^{\mathrm{h}}\right] \cdot \mathbf{v}_{\mathrm{m}}^{\mathrm{h}}\right)_{\mathscr{T}_{\mathrm{h}}} - \left(\mathrm{Grad}q, J_{\mathrm{m}}^{\mathrm{h}}\mathbf{F}_{\mathrm{m}}^{-1}\mathbf{v}_{\mathrm{f}}^{\mathrm{h}}\right)_{\mathscr{T}_{\mathrm{h}}} + \left\langle q, J_{\mathrm{m}}^{\mathrm{h}}\widehat{\mathbf{v}}_{\mathrm{f}}^{\mathrm{h}} \cdot \mathbf{F}_{\mathrm{m}}^{-\mathsf{T}}\mathbf{n}_{\mathrm{f}}\right\rangle_{\partial\mathscr{T}_{\mathrm{h}}} = 0, \tag{22c}$$

$$\left\langle \eta, J_{\mathrm{m}}^{\mathrm{h}}\widehat{\mathbf{T}}_{\mathrm{f}}^{\mathrm{h}}\mathbf{F}_{\mathrm{m}}^{-\mathsf{T}}\mathbf{n}_{\mathrm{f}}\right\rangle_{\partial\mathscr{T}_{\mathrm{h}}\setminus\partial\Omega_{D_{\mathrm{F}}}} \left\langle \eta, J_{\mathrm{m}}^{\mathrm{h}}\breve{\mathbf{T}}_{\mathrm{f}}^{\mathrm{h}}\mathbf{F}_{\mathrm{m}}^{-\mathsf{T}}\mathbf{n}_{\mathrm{f}}\right\rangle_{\partial\Omega_{O_{\mathrm{F}}}} - \left\langle \eta, J_{\mathrm{m}}^{\mathrm{h}}\mathbf{g}_N\right\rangle_{\partial\Omega_{N_{\mathrm{F}}}} = 0, \tag{22d}$$

$$\left\langle \eta, J_{\mathrm{m}}^{\mathrm{h}}\widehat{\mathbf{v}}_{\mathrm{f}}^{\mathrm{h}}\right\rangle_{\partial\Omega_{D_{\mathrm{F}}}} - \left\langle \eta, J_{\mathrm{m}}^{\mathrm{h}}\mathbf{g}_{D_{\mathrm{F}}}\right\rangle_{\partial\Omega_{D_{\mathrm{F}}}} = 0, \tag{22e}$$

where $\widehat{\mathbf{T}}_{\mathrm{f}}^{\mathrm{h}}\mathbf{F}_{\mathrm{m}}^{-\mathsf{T}}\mathbf{n}_{\mathrm{f}}$ *is defined in Eq.* (17) *and* $\breve{\mathbf{T}}_{\mathrm{f}}^{\mathrm{h}}\mathbf{F}_{\mathrm{m}}^{-\mathsf{T}}\mathbf{n}_{\mathrm{f}}$ *is defined as*

$$\breve{\mathbf{T}}_{\mathrm{f}}^{\mathrm{h}}\mathbf{F}_{\mathrm{m}}^{-\mathsf{T}}\mathbf{n}_{\mathrm{f}} := \left[-\mu_{\mathrm{f}}\breve{\mathbf{L}}_{\mathrm{f}}^{\mathrm{h}} + \breve{p}_{\mathrm{f}}^{\mathrm{h}}\mathbf{I}\right]\mathbf{F}_{\mathrm{m}}^{-\mathsf{T}}\breve{\mathbf{n}}_{\mathrm{f}} + \mathbf{S}_{\mathrm{f}}\left(\breve{\mathbf{v}}_{\mathrm{f}}^{\mathrm{h}} - \widehat{\mathbf{v}}_{\mathrm{f}}^{\mathrm{h}}\right). \tag{23}$$

Subproblem 1.2 (Mesh Motion)

$$\left(\mathbf{C}, \mathbf{F}_{\mathrm{m}}^{\mathrm{h}} - \mathbf{I}\right)_{\mathscr{T}_{\mathrm{h}}} - \left(\mathbf{C}, \mathrm{Grad}\,\mathbf{u}_{\mathrm{m}}^{\mathrm{h}}\right)_{\mathscr{T}_{\mathrm{h}}} - \left\langle \mathbf{C}\mathbf{n}_{\mathrm{m}}, \left(\mathbf{u}_{\mathrm{m}}^{\mathrm{h}} - \widehat{\mathbf{u}}_{\mathrm{m}}^{\mathrm{h}}\right)\right\rangle_{\partial\mathscr{T}_{\mathrm{h}}} = 0, \tag{24a}$$

$$\left(\mathrm{Grad}\,\mathbf{w}, \mathbb{C}\left[\mathrm{Sym}\mathbf{F}_{\mathrm{m}}^{\mathrm{h}} - \mathbf{I}\right]\right)_{\mathscr{T}_{\mathrm{h}}} - \left\langle \mathbf{w}, \widehat{\mathbf{P}}_{\mathrm{m}}^{\mathrm{h}}\mathbf{n}_{\mathrm{m}}\right\rangle_{\partial\mathscr{T}_{\mathrm{h}}} = (\mathbf{w}, \mathbf{b}_{\mathrm{m}})_{\mathscr{T}_{\mathrm{h}}}, \tag{24b}$$

$$\left\langle \omega, \widehat{\mathbf{P}}_{\mathrm{m}}^{\mathrm{h}}\mathbf{n}_{\mathrm{m}}\right\rangle_{\partial\mathscr{T}_{\mathrm{h}}\setminus\partial\Omega_{D_{\mathrm{F}}}} + \left\langle \omega, \breve{\mathbf{P}}_{\mathrm{m}}^{\mathrm{h}}\mathbf{n}_{\mathrm{m}}\right\rangle_{\partial\Omega_{O_{\mathrm{F}}}} = \left\langle \omega, \mathbf{t}_{N_{\mathrm{m}}}\right\rangle_{\partial\Omega_{N_{\mathrm{F}}}}, \tag{24c}$$

$$\left\langle \omega, \widehat{\mathbf{u}}_{\mathrm{m}}^{\mathrm{h}}\right\rangle_{\partial\Omega_{D_{\mathrm{F}}}} = \left\langle \omega, \bar{\mathbf{u}}_{D_{\mathrm{m}}}\right\rangle_{\partial\Omega_{D_{\mathrm{F}}}}, \tag{24d}$$

where $\widehat{\mathbf{P}}_{\mathrm{m}}^{\mathrm{h}}\mathbf{n}_{\mathrm{m}}$ *is defined in Eq.* (19) *and* $\breve{\mathbf{P}}_{\mathrm{m}}^{\mathrm{h}}\mathbf{n}_{\mathrm{m}}$ *is defined as*

$$\breve{\mathbf{P}}_{\mathrm{m}}^{\mathrm{h}}\mathbf{n}_{\mathrm{m}} := \mathbb{C}\left(\mathrm{Sym}\breve{\mathbf{F}}_{\mathrm{m}}^{\mathrm{h}} - \mathbf{I}\right)\breve{\mathbf{n}}_{\mathrm{m}} - \mathbf{S}_{\mathrm{m}}\left(\breve{\mathbf{u}}_{\mathrm{m}}^{\mathrm{h}} - \widehat{\mathbf{u}}_{\mathrm{m}}^{\mathrm{h}}\right). \tag{25}$$

$\forall\,(\mathbf{G}, \mathbf{y}, q, \eta, \mathbf{C}, \mathbf{w}, \omega) \in \mathscr{G}_{\mathrm{h}} \times \mathscr{Y}_{\mathrm{h}} \times \mathscr{P}_{\mathrm{h}} \times \mathscr{N}_{\mathrm{h}} \times \mathscr{C}_{\mathrm{h}} \times \mathscr{U}_{\mathrm{h}} \times \mathscr{M}_{\mathrm{h}}$,

where $\partial\Omega_{D_{\mathrm{F}}} = \bigcup_{i=1}^{N} \partial\Omega_{D_{\mathrm{F}}}^{i}$, $\partial\Omega_{N_{\mathrm{F}}} = \bigcup_{i=1}^{N} \partial\Omega_{N_{\mathrm{F}}}^{i}$, and $\partial\Omega_{O_{\mathrm{F}}} = \bigcup_{i=1}^{N} \partial\Omega_{O_{\mathrm{F}}}^{i}$. Eqs. (23) and (25) show that all the local fields are donated from a mesh that is different from the one where the corresponding integral is being computed.

C. Implementation

The solution of Problem 1 is achieved through the Newton-Raphson method [27]. This method linearly approximates the residual of the nonlinear system allowing for the solution to be updated in an iterative fashion. The resulting linear system for a general overset mesh configuration is of the form

$$\begin{bmatrix} \mathcal{A} & \mathcal{B} \\ \mathcal{C} & \mathcal{D} \end{bmatrix} \begin{Bmatrix} \Upsilon \\ \Lambda \end{Bmatrix} = \begin{Bmatrix} \mathcal{H} \\ \mathcal{Q} \end{Bmatrix}, \tag{26}$$

where $\mathcal{A}$, $\mathcal{B}$, $\mathcal{C}$, $\mathcal{D}$ are block matrices and Υ, Λ, $\mathcal{H}$, $\mathcal{Q}$ are block vectors at each Newton iteration. For example,

$$\mathcal{A} := \begin{bmatrix} A^1 & 0 & \cdots & 0 \\ 0 & A^2 & \cdots & \vdots \\ 0 & \cdots & \ddots & 0 \\ 0 & \cdots & 0 & A^N \end{bmatrix}. \tag{27}$$

The matrix $\mathcal{A}$ is a block diagonal matrix and each A^i is also a block diagonal matrix for the i^{th} mesh because the coupling between the entries in A^i only occurs within each $K \in \mathcal{T}_{\mathrm{h}}^{i}$, but not across neighboring elements because of the discontinuous basis functions used. Each block is representative of different degree of freedom coupling for the HDG formulation, namely,

$$\begin{bmatrix} \mathrm{VVC} & \mathrm{VFC} \\ \mathrm{FVC} & \mathrm{FFC} \end{bmatrix} \begin{Bmatrix} \text{local solution} \\ \text{global solution} \end{Bmatrix} = \begin{Bmatrix} \text{local source} \\ \text{global source} \end{Bmatrix}, \tag{28}$$

where V is volume, F is face, and C is coupling. In Section III.A we discussed that the coupling between meshes is a FVC, which corresponds to the $\mathcal{C}$ block matrix. In addition to the overset coupling in the $\mathcal{C}$ matrix we also have some extra FFC, the $\mathcal{D}$ matrix, which can be seen in the integrals associated with Eqs. (23) and (25). This extra FFC does not help tie the meshes together, but instead is a byproduct of the chosen numerical flux that enforces that the hybrid fields, fluid velocity and mesh displacement, are continuous across element boundaries. Overall, the structure of the linear system does not change for an overset configuration compared to a single mesh configuration. This implies that we can use the same linear algebra techniques that is common for the HDG method. Through static condensation [28], the local solution is condensed out of the linear system via the Schur complement [29] in order to obtain a system in terms of the global unknowns only,

$$\left(\mathcal{D} - \mathcal{C}\mathcal{A}^{-1}\mathcal{B}\right)\Lambda = \mathcal{Q} - \mathcal{C}\mathcal{A}^{-1}\mathcal{H}. \tag{29}$$

Since $\mathcal{A}$ is block diagonal it is easily inveritable. Solving Eq. (29) provides us with the global solution $\Lambda = \left\{\widehat{\mathbf{v}}_{\mathrm{f}}^{\mathrm{h}} \quad \widehat{\mathbf{u}}_{\mathrm{m}}^{\mathrm{h}}\right\}^{\mathsf{T}}$. The global solution is then used to compute the local solution via

$$\Upsilon^i = \left(\mathcal{A}^i\right)^{-1}\left(\mathcal{H}^i - \mathcal{B}^i\Lambda^i\right), \tag{30}$$

on a cell-by-cell basis for each $K \in \mathcal{T}_{\mathrm{h}}^i$ for each mesh $i = 1, \ldots, N$. We have implemented the overset coupling algorithm that is described in more detail in Kauffman et al. [2], and have utilized a sparse-direct linear solver `UMFPACK` [30] to obtain the global solution through the `deal.II` finite element library [31].

IV. Computational Studies

Problem 1 is the full isentropic ALE Navier-Stokes formulation. In terms of overset meshes this formulation allows individual meshes to deform and meshes to move relative to one another. This implies that meshes surrounding a body do not need to deform as bodies move, which maintains the initial mesh quality. Two-dimensional verification, through the method of manufactured solutions [32], of Problem 1 shows optimal order convergence for varying degrees and arbitrary amount of overlap in a four overset mesh system for varying approximation orders.

A. Two-dimensional verification

For the two-dimensional manufactured solution [32] of Problem 1 the velocity field is chosen as

$$\mathbf{v}^e\left(\mathbf{X}\right) = \begin{pmatrix}\cos\left(\pi\left[x+y\right]\right)\sin\left(\pi\left[x-y\right]\right)\cos\left(\frac{\pi}{4}t\right)\\ \cos\left(\pi\left[x+y\right]\right)\sin\left(\pi\left[x-y\right]\right)\cos\left(\frac{\pi}{4}t\right)\end{pmatrix}, \tag{31}$$

the pressure is chosen as

$$p^e\left(\mathbf{X}\right) = \frac{\cos\left(\pi\left[x+y\right]\right)\sin\left(\pi\left[x-y\right]\right)\cos\left(\frac{\pi}{4}t\right)}{\varepsilon}, \tag{32}$$

and the displacement is chosen as

$$\mathbf{u}^e\left(\mathbf{X}\right) = \begin{pmatrix}-x - \sin\left(\frac{\pi}{4}\left[x-y\right]\right)\cos\left(\frac{\pi}{4}t\right)\\ -y + \cos\left(\frac{\pi}{4}\left[x+y\right]\right)\cos\left(\frac{\pi}{4}t\right)\end{pmatrix}. \tag{33}$$

The velocity gradient is defined as $\mathbf{L}^e := \mathrm{Grad}\mathbf{v}^e\mathbf{F}^{-1}$ from Eq. (6a) and the deformation gradient is defined as $\mathbf{F}^e := \mathrm{Grad}\mathbf{u}^e + \mathbf{I}$ from Eq. (7a). In this formulation, because the pressure is chosen arbitrarily it is necessary to compute a right-hand-side term in Eq. (6c). The right-hand-side terms are not presented here but can be calculated using a symbolic algebra package. Fig. 2 shows the computational domain under investigation for the ALE verification problem. Note that because of the choice of the displacement field, care must be taken so that the determinant of the deformation gradient is not zero anywhere in the domain. The values of the parameters $\{\varepsilon, \rho_{\mathrm{f}}, \mu_{\mathrm{f}}, \lambda_{\mathrm{m}}, \mu_{\mathrm{m}}, \Delta t\}$ are chosen to be $\left\{1\ \left[\mathrm{m}\cdot\mathrm{s}^2/\mathrm{kg}\right],\ 1\ \left[\mathrm{kg}/\mathrm{m}^3\right],\ 1/2\ [\mathrm{Pa}\cdot\mathrm{s}],\ 1\ [\mathrm{Pa}],\ 1/2\ [\mathrm{Pa}],\ 10^{-6}\ [\mathrm{s}]\right\}$. Fig. 3 shows the four overset mesh system that is used in the verification of Problem 1. Table 2 describes the mesh domains, initial cell size and corresponding color in Fig. 3.

Table 2 Domain definitions and initial minimum cell sizes for all four meshes used for the verification of Problem 1. The set of points given for Ω^1 – Ω^4 correspond to lower left and upper right corners respectively.

Mesh	Fig. 3 Color	Domain	h_0
Ω^1	Orange	$[0.5, 0.5] \times [1.1, 1.1]$	0.2121
Ω^2	Green	$[0.8, 0.8] \times [1.5, 1.5]$	0.2475
Ω^3	Blue	$[0.5, 0.7] \times [1.2, 1.5]$	0.2658
Ω^4	Red	$[0.9, 0.5] \times [1.5, 1]$	0.1953

Convergence rates are demonstrated using the L^2 error norm, defined as

$$\|\mathbf{a}\|_{L^2} := \sqrt{\int_\Omega \mathbf{a}\cdot\mathbf{a}\, d\Omega}, \tag{34}$$

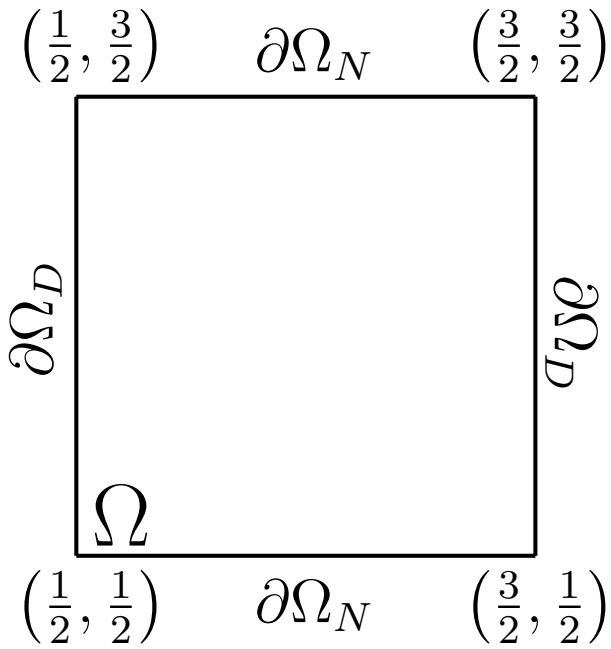

Fig. 2 Computational domain used for the two-dimensional verification of isentropic ALE Navier-Stokes with corresponding boundary conditions.

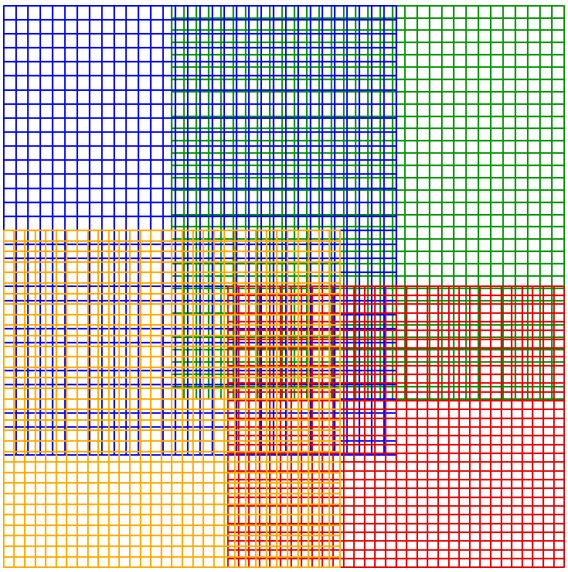

Fig. 3 The four overset mesh system used for the two-dimensional verification of isentropic ALE Navier-Stokes simulations.

for a generic vector field **a**. Similar definitions exist for scalar fields and tensor fields. Fig. 4 shows the convergence results for all of the linear elastic fields that govern the mesh motion: displacement and the deformation gradient. Both fields converge at the optimal rate for all approximation orders ($k = 1, \ldots, 4$) for each mesh. Fig. 5 shows the convergence results for all of the fluid fields: velocity, pressure, and velocity gradient. All fields converge at the optimal rate for all approximation orders ($k = 1, \ldots, 4$) for each mesh. The error in the velocity gradient for Ω^1 and Ω^4 starts to increase on the finest level mesh. This is attributed to the third order temporal scheme starting to dominate the error.

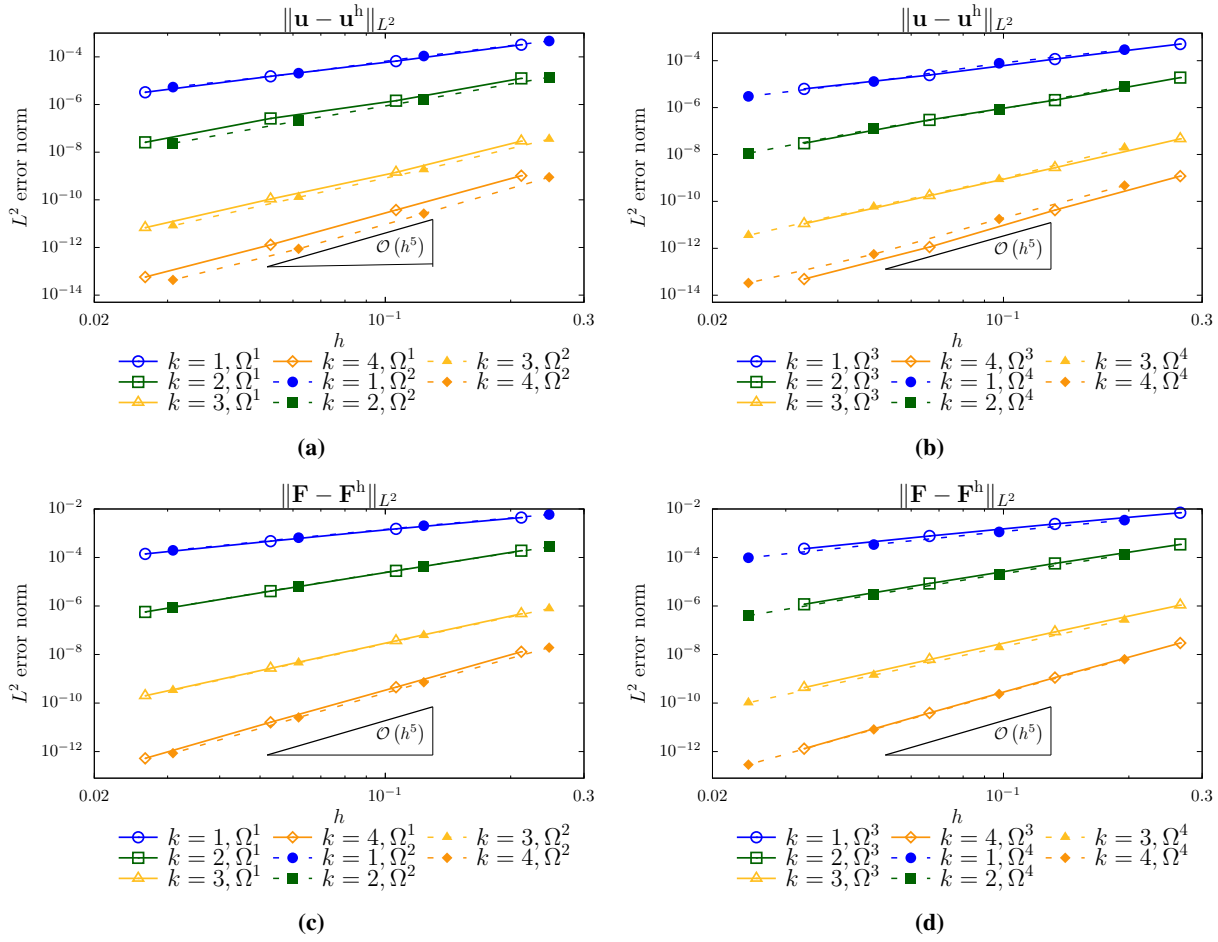

Fig. 4 Convergence results of the displacement u (a) and (b) and the deformation gradient F (c) and (d). All fields show optimal order convergence for all approximation orders. Note that this also verifies the overset system for the two-field linear elasticity problem, since no fluid properties affect this system.

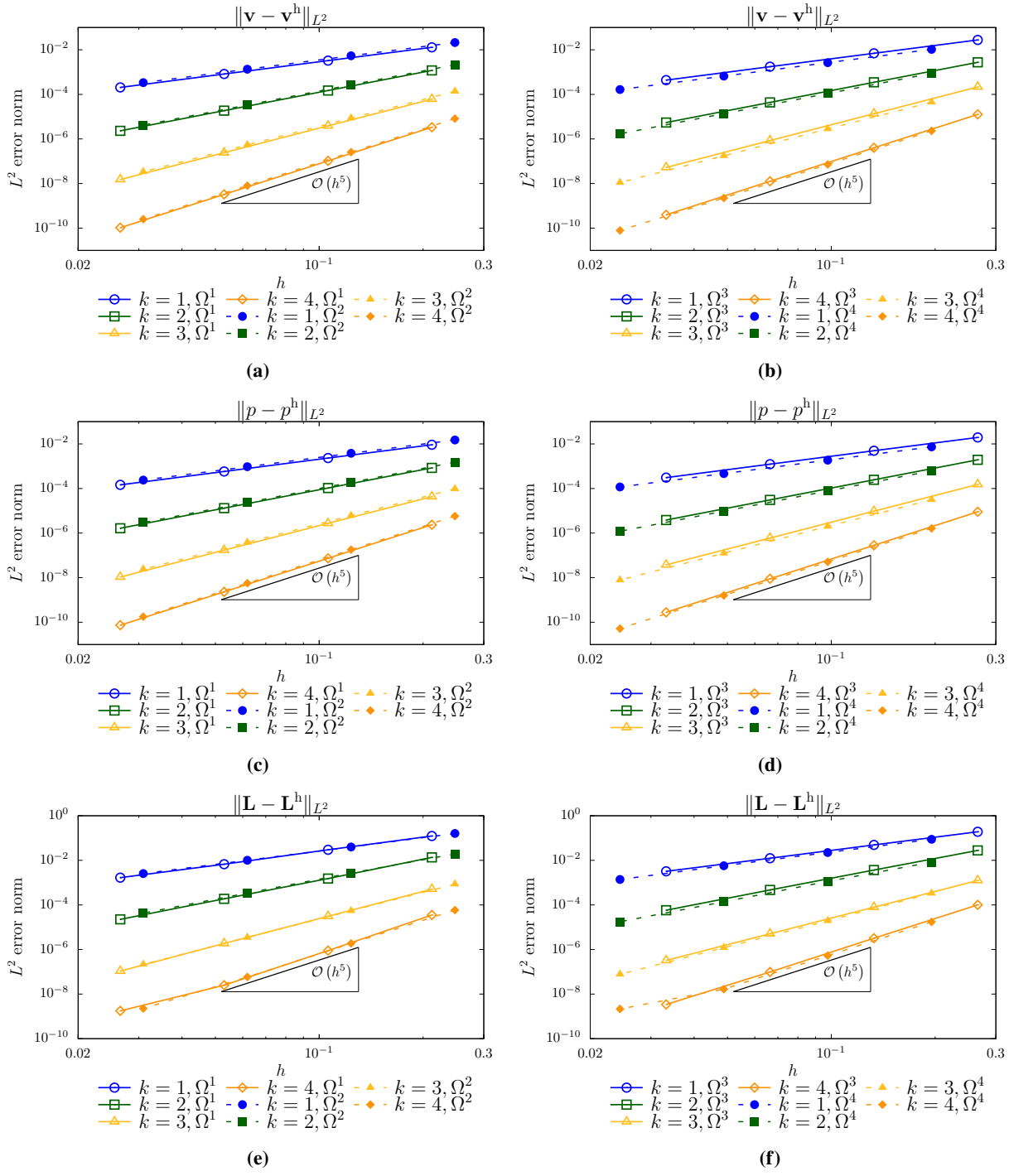

Fig. 5 Convergence results of the velocity v (a) and (b), the pressure p (c) and (d), and the velocity gradient L (e) and (f). All fields show optimal order convergence for all approximation orders. For $k = 4$ there is a slight deviation in the velocity gradient from the optimal slope. This is attributed to the temporal error dominating at the finest level mesh.

V. Summary

We have presented an overset-HDG method for an isentropic ALE Navier-Stokes formulation, which we have verified through the method of manufactured solutions in two-dimensions. Through verification, all fields, on each mesh, of the coupled system converged at optimal order $\mathcal{O}(k+1)$, where k is the approximation order. Through this verification procedure we have demonstrated that the amount of overlap between meshes is arbitrary and that convergence is optimal even for higher-order approximations.

VI. Future Work

The extensions of this work are to develop a parallel communication algorithm and implement a general block parallel solver. The parallelization of the communication algorithm will allow for more realistic simulations to be performed and direct comparisons between model experiments and other accepted overset methods. We expect that the general trend in the scaling between a single mesh configuration and a general N-mesh overset configuration will be similar once the communication algorithm is fully parallelized and a more robust linear solver is implemented. We are not expecting any overset configuration to run faster than a single mesh configuration. We will directly compare our fully parallel overset-HDG algorithm to existing overset codes already in use, and we expect that our algorithm will outperform the current overset standards.

Appendix

The fully discrete local weak formulation is presented below. This takes into account the third order backward difference formula (BDF3), defined in Eq. (21), used to discretize the Local Problem 1 in time. We also include the backward difference approximation we use to calculate the mesh velocity. For increased clarity the superscript h for all fields is removed and replaced with superscript n to indicate the current timestep. Note that $n-1$ refers to the previous timestep, and so on. So at timestep n the fully discrete weak form is

Local Problem 2 (Local Isentropic ALE Navier-Stokes) *Find* $\left(\mathbf{L}_{\mathrm{f}}^{n}, \mathbf{v}_{\mathrm{f}}^{n}, p_{\mathrm{f}}^{n}, \mathbf{F}_{\mathrm{m}}^{n}, \mathbf{u}_{\mathrm{m}}^{n}\right) \in \mathscr{G}_{\mathrm{h}} \times \mathscr{V}_{\mathrm{h}} \times \mathscr{P}_{\mathrm{h}} \times \mathscr{C}_{\mathrm{h}} \times \mathscr{U}_{\mathrm{h}}$ *such that*

Local Subproblem 2.1 (Fluid)

$$\left(\mathbf{G}, J_{\mathrm{m}}^{n}\mathbf{L}_{\mathrm{f}}^{n}\right)_{K} - \left(\mathbf{G}, J_{\mathrm{m}}^{n}\mathrm{Grad}\mathbf{v}_{\mathrm{f}}^{n}\left[\mathbf{F}_{\mathrm{m}}^{n}\right]^{-1}\right)_{K} + \left\langle \mathbf{G}, J_{\mathrm{m}}^{n}\left(\mathbf{v}_{\mathrm{f}}^{n} - \widehat{\mathbf{v}}_{\mathrm{f}}^{n}\right) \otimes \left[\mathbf{F}_{\mathrm{m}}^{n}\right]^{-\mathsf{T}}\mathbf{n}_{\mathrm{f}}\right\rangle_{\partial K} = 0, \tag{35a}$$

$$\begin{aligned}\left(\mathbf{y}, \frac{J_{\mathrm{m}}^{n}\rho_{\mathrm{f}}}{6\Delta t}\left[11\mathbf{v}_{\mathrm{f}}^{n} - 18\mathbf{v}_{\mathrm{f}}^{n-1} + 9\mathbf{v}_{\mathrm{f}}^{n-2} - 2\mathbf{v}_{\mathrm{f}}^{n-3}\right]\right)_{K} + \left(\mathbf{y}, J_{\mathrm{m}}^{n}\rho_{\mathrm{f}}\mathbf{L}_{\mathrm{f}}^{n}\left[\mathbf{v}_{\mathrm{f}}^{\mathrm{h}} - \left\{\frac{\mathbf{u}_{\mathrm{m}}^{n} - \mathbf{u}_{\mathrm{m}}^{n-1}}{\Delta t}\right\}\right]\right)_{K} \\ + \left(\mathrm{Grad}\mathbf{y}, J_{\mathrm{m}}^{n}\left[\mu_{\mathrm{f}}\mathbf{L}_{\mathrm{f}}^{n} - p_{\mathrm{f}}^{n}\mathbf{I}\right]\left[\mathbf{F}_{\mathrm{m}}^{n}\right]^{-\mathsf{T}}\right)_{K} + \left(\mathbf{y}, J_{\mathrm{m}}^{n}\rho_{\mathrm{f}}\left[\mathrm{Grad}\mathbf{v}_{\mathrm{f}}^{n} : \left[\mathbf{F}_{\mathrm{m}}^{n}\right]^{-\mathsf{T}}\right]\mathbf{v}_{\mathrm{f}}^{n}\right)_{K} \\ + \left\langle \mathbf{y}, J_{\mathrm{m}}^{n}\widehat{\mathbf{T}}_{\mathrm{f}}^{n}\left[\mathbf{F}_{\mathrm{m}}^{n}\right]^{-\mathsf{T}}\mathbf{n}_{\mathrm{f}}\right\rangle_{\partial K} = \left(\mathbf{y}, J_{\mathrm{m}}^{n}\mathbf{f}_{\mathrm{f}}^{n}\right)_{K},\end{aligned} \tag{35b}$$

$$\begin{aligned}\left(q, \frac{J_{\mathrm{m}}^{n}\varepsilon}{6\Delta t}\left[11p_{\mathrm{f}}^{n} - 18p_{\mathrm{f}}^{n-1} + 9p_{\mathrm{f}}^{n-2} - 2p_{\mathrm{f}}^{n-3}\right]\right)_{K} + \left(q, J_{\mathrm{m}}^{n}\varepsilon\left\{\left[\mathbf{F}_{\mathrm{m}}^{n}\right]^{-\mathsf{T}}\mathrm{Grad}p_{\mathrm{f}}^{n}\right\} \cdot \left\{\frac{\mathbf{u}_{\mathrm{m}}^{n} - \mathbf{u}_{\mathrm{m}}^{n-1}}{\Delta t}\right\}\right)_{K} \\ - \left(\mathrm{Grad}q, J_{\mathrm{m}}^{n}\left[\mathbf{F}_{\mathrm{m}}^{n}\right]^{-1}\mathbf{v}_{\mathrm{f}}^{\mathrm{h}}\right)_{K} + \left\langle q, J_{\mathrm{m}}^{n}\widehat{\mathbf{v}}_{\mathrm{f}}^{n} \cdot \left[\mathbf{F}_{\mathrm{m}}^{n}\right]^{-\mathsf{T}}\mathbf{n}_{\mathrm{f}}\right\rangle_{\partial K} = 0,\end{aligned} \tag{35c}$$

where

$$\widehat{\mathbf{T}}_{\mathrm{f}}^{n}\left[\mathbf{F}_{\mathrm{m}}^{n}\right]^{-\mathsf{T}}\mathbf{n}_{\mathrm{f}} := \left[-\mu_{\mathrm{f}}\mathbf{L}_{\mathrm{f}}^{n} + p_{\mathrm{f}}^{n}\mathbf{I}\right]\left[\mathbf{F}_{\mathrm{m}}^{n}\right]^{-\mathsf{T}}\mathbf{n}_{\mathrm{f}} + \mathbf{S}_{\mathrm{f}}^{n}\left(\mathbf{v}_{\mathrm{f}}^{n} - \widehat{\mathbf{v}}_{\mathrm{f}}^{n}\right), \tag{36}$$

Local Subproblem 2.2 (Mesh Motion)

$$\left(\mathbf{C}, \mathbf{F}_{\mathrm{m}}^{n} - \mathbf{I}\right)_{K} - \left(\mathbf{C}, \mathrm{Grad}\mathbf{u}_{\mathrm{m}}^{n}\right)_{K} - \left\langle \mathbf{C}\mathbf{n}_{\mathrm{m}}, \left(\mathbf{u}_{\mathrm{m}}^{n} - \widehat{\mathbf{u}}_{\mathrm{m}}^{n}\right)\right\rangle_{\partial K} = 0, \tag{37a}$$

$$\left(\mathrm{Grad}\mathbf{w}, \mathbb{C}\left[\mathrm{Sym}\mathbf{F}_{\mathrm{m}}^{n} - \mathbf{I}\right]\right)_{K} - \left\langle \mathbf{w}, \widehat{\mathbf{P}}_{\mathrm{m}}^{n}\mathbf{n}_{\mathrm{m}}\right\rangle_{\partial K} = \left(\mathbf{w}, \mathbf{b}_{\mathrm{m}}^{n}\right)_{K}, \tag{37b}$$

where

$$\widehat{\mathbf{P}}_{\mathrm{m}}^{n}\mathbf{n}_{\mathrm{m}} := \mathbb{C}\left(\mathrm{Sym}\mathbf{F}_{\mathrm{m}}^{n} - \mathbf{I}\right)\mathbf{n}_{\mathrm{m}} - \mathbf{S}_{\mathrm{m}}\left(\mathbf{u}_{\mathrm{m}}^{n} - \widehat{\mathbf{u}}_{\mathrm{m}}^{n}\right), \tag{38}$$

$\forall\, (\mathbf{G}, \mathbf{y}, q, \mathbf{C}, \mathbf{w}) \in \mathscr{G}_\mathrm{h} \times \mathscr{Y}_\mathrm{h} \times \mathscr{P}_\mathrm{h} \times \mathscr{C}_\mathrm{h} \times \mathscr{U}_\mathrm{h}$,

where $\mathbf{S}_\mathrm{f}^n$ is defined as

$$\mathbf{S}_\mathrm{f}^n := \left(2\mu_\mathrm{f} + \rho_\mathrm{f}\|\mathbf{v}_\mathrm{f}^{n-1}\|\right)\mathbf{I}. \tag{39}$$

Acknowledgments

J. Kauffman gratefully acknowledges financial support from the Applied Research Laboratory Walker Graduate Assistantship and the National Research Council postdoctoral fellowship.

References

[1] Sheldon, J. P., Miller, S. T., and Pitt, J. S., "A hybridizable discontinuous Galerkin method for modeling fluid–structure interaction," *Journal of Computational Physics*, Vol. 326, 2016, pp. 91–114.

[2] Kauffman, J. A., Sheldon, J. P., and Miller, S. T., "Overset meshing coupled with hybridizable discontinuous Galerkin finite elements," *International Journal for Numerical Methods in Engineering*, 2017. URL `http://dx.doi.org/10.1002/nme.5512`.

[3] Chan, W. M., "Overset grid technology development at NASA Ames Research Center," *Computer & Fluids*, Vol. 38, 2009, pp. 496–503.

[4] Sherer, S. E., Visbal, M. R., and Galbraith, M. C., "Automated Preprocessing Tools for Use with a High–Order Overset–Grid Algorithm," 44^{th} *AIAA Aerospace Sciences Meeting and Exhibit*, Vol. Overset and Adaptive Grids, Reno, Nevada, 2006, pp. 13–30.

[5] Bodony, D. J., Zagaris, G., Reichert, A., and Zhang, Q., "Provably stable overset grid methods for computational aeroacoustics," *Journal of Sound and Vibration*, Vol. 330, 2011, pp. 4161–4179.

[6] Noack, R. W., "SUGGAR: a General Capability for Moving Body Overset Grid Assembly," 17^{th} *AIAA Computational Fluid Dynamics Conference*, Vol. Overset Grids, Toronto, Ontario, Canada, 2005, pp. 5117–5138.

[7] Noack, R. W., Boger, D. A., Kunz, R. F., and Carrica, P. M., "Suggar++: An Improved General Overset Grid Assembly Capability," 19^{th} *AIAA Computational Fluid Dynamics*, Vol. Overset Grid Methods and Grid Refinement and Deformation Schemes, San Antonio, TX, 2009, pp. 3992–4040.

[8] Abras, J. N., Lynch, C. E., and Smith, M. J., "Computational Fluid Dynamics–Computational Structural Dynamics Rotor Coupling Using an Unstructured Reynolds–Averaged Navier–Stokes Methodology," *Journal of the American Helicopter Society*, Vol. 57, 2012, pp. 1–14.

[9] Foster, N. F., and Noack, R. W., "High–Order Overset Interpolation within an OVERFLOW Solution," 50^{th} *AIAA Aerospace Sciences Meeting including the New Horizons Forum and Aerospace Expostion*, Vol. High-order Methods on Unstructured Grids III, Nashville, TN, 2012, pp. 728–736.

[10] Clark, C. G., Lyons, D. G., and Neu, W. L., "Comparison of Single and Overset Grid Techniques for CFD Simulations of a Surface Effect Ship," *ASME 2014* 33^{rd} *International Conference on Ocean, Offshore and Arctic Engineering*, Vol. CFD and VIV, San Francisco, CA, 2014, pp. 24207–24214.

[11] Östman, A., Pakozdi, C., Sileo, L., Stansberg, C.-T., and de Carvalho e Silva, D. F., "A Fully Nonliner RANS–VOF Numerical Wavetank Applied in the Analysis of Green Water on FPSO in Waves," *ASME*33^{rd} *International Conference on Ocean, Offshore and Arctic Engineering*, Vol. Ocean Engineering, San Francisco, CA, 2014, pp. 23927–23935.

[12] Field, P. L., and Neu, W. L., "Comparison of RANS and Potential Flow Force Comutations for one DOF Heave and Pitch of the ONR Tumblehome Hullform," *ASME 2013* 32^{nd} *International Conference on Ocean, Offshore and Arctic Engineering*, Vol. Marine Hydrodynamics, Nantes, France, 2013, pp. 10562–10572.

[13] Sengupta, T. K., Suman, V., and Singh, N., "Solving Navier–Stokes equation for flow past cylinders using single–block structured and overset grids," *Journal of Computational Physics*, Vol. 229, 2010, pp. 178–199.

[14] Nastase, C., Mavriplis, D., and Sitaraman, J., "An overset unstructured mesh discontinuous Galerkin approach for aerodynamic problems," *49th AIAA Aerospace Sciences Meeting including the New Horizons Forum and Aerospace Exposition*, 2011, p. 195.

[15] Galbraith, M. C., Benek, J. A., Orkwis, P. D., and Turner, M. G., "A Discontinuous Galerkin Chimera scheme," *Computers & Fluids*, Vol. 98, 2014, pp. 27–53.

[16] Brazell, M. J., Sitaraman, J., and Mavriplis, D. J., "An overset mesh approach for 3D mixed element high-order discretizations," *Journal of Computational Physics*, Vol. 322, 2016, pp. 33–51.

[17] Cockburn, B., Gopalakrishnan, J., and Lazarov, R., "Unified Hybridization of Discontinuous Galerkin, Mixed, and Continuous Galerkin Methods for Second Order Elliptic Problems," *SIAM Journal on Numerical Analysis*, Vol. 47, 2009, pp. 1319–1365.

[18] Nguyen, N., and Peraire, J., "Hybridizable discontinuous Galerkin method for partial differential equations in continuum mechanics," *Journal of Computational Physics*, Vol. 231, 2012, pp. 5955–5988.

[19] Fidkowski, K. J., "A hybridized discontinuous Galerkin method on mapped deforming domains," *Computers & Fluids*, Vol. 139, 2016, pp. 80–91.

[20] Ahnert, T., and Bärwolff, G., "Numerical comparison of hybridizable discontinuous Galerkin and finite volume methods for incompressible flow," *Internaltional Journal for Numerical Methods in Flu*, Vol. 76, 2014, pp. 267–281.

[21] Ciarlet, P. G., "The finite element method for elliptic problems," *Classics in applied mathematics*, Vol. 40, 2002, pp. 1–511.

[22] Bagwell, T. G., "CFD Simulation of Flow Tones from Grazing Flow Past a Deep Cavity," *ASME International Mechanical Engineering Congress and Exposition*, American Society of Mechanical Engineers, 2006, pp. 105–114.

[23] Holzapfel, G. A., *Nonlinear Solid Mechanics: A Continuum Approach for Engineering*, John Wiley & Sons, LTD, New York, 2000.

[24] Gurtin, M. E., Fried, E., and Anand, L., *The Mechanics and Thermodynamics of Continua*, Cambridge University Press, New York, 2010.

[25] Donea, J., Huerta, A., Ponthot, J., and Rodriguez-Ferran, A., "Arbitrary Lagrangian Eulerian methods," *Fundamentals in Encyclopedia of Computational Mechanics*, Vol. 1, edited by E. Stein, R. de Borst, and T. J. Hughes, Wiley, New York, 2004, Chap. 14, pp. 413–437.

[26] Süli, E., and Mayers, D. F., *An introduction to Numerical Analysis*, Cambridge university press, 2003.

[27] Quarteroni, A., Sacco, R., and Saleri, F., *Numerical Mathematics*, Springer, 2000.

[28] Felippa, C. A., *Introduction to finite element methods*, Department of Aerospace Engineering Sciences, University of Colorado at Boulder, 2015. Accessed: 2016-01-15.

[29] Zhang, F., *The Schur complement and its applications*, Vol. 4, Springer Science & Business Media, 2005.

[30] Davis, T., "Algorithm 832: UMFPACK V4. 3—an unsymmetric-pattern multifrontal method," *ACM Transactions on Mathematical Software (TOMS)*, Vol. 30, No. 2, 2004, pp. 196–199.

[31] Alzetta, G., Arndt, D., Bangerth, W., Boddu, V., Brands, B., Davydov, D., Gassmoeller, R., Heister, T., Heltai, L., Kormann, K., Kronbichler, M., Maier, M., Pelteret, J., Turcksin, B., and Wells, D., "The `deal.II` Library, Version 9.0," *Journal of Numerical Mathematics*, 2018, accepted.

[32] Salari, K., and Knupp, P., "Code verification by the method of manufactured solutions," Tech. rep., Sandia National Labs., Albuquerque, NM (US); Sandia National Labs., Livermore, CA (US), 2000.